Beam Dynamics Measurements for the SLAC Laser Acceleration Experiment*

E. Colby, R. Ischebeck, D. McCormick, C. McGuinness, J. Nelson, R. Noble, C. Sears,
R. Siemann, J. Spencer†, SLAC, Menlo Park, CA 94025, USA
T. Plettner, Stanford University, Stanford, CA 94305, USA

Abstract

The NLC Test Accelerator (NLCTA) was built to address beam dynamics issues for the Next Linear Collider and beyond. An S-Band RF gun, diagnostics and low energy spectrometer (LES) at 6 MeV together with a large-angle extraction line at 60 MeV have now been built and commissioned for the laser acceleration experiment, E163. Following a four quad matching section after the NLCTA chicane, the extraction section is followed by another matching section, final focus and buncher. The laser-electron interaction point (IP) is followed by a broad range, high resolving power spectrometer (HES) for electron bunch analysis. Optical symmetries in the design of the 25.5° extraction line provide 1:1 phase space transfer without sextupoles for a large, 6D phase space volume and range of input conditions. Spot sizes down to a few microns at the IP (HES object) allow testing microscale structures with high resolving power at the HES image. Tolerances, tuning sensitivities, diagnostics and the latest commissioning results are discussed and compared to design expectations.

INTRODUCTION

Because the NLCTA[**?**] is an existing facility, many constraints had to be accommodated as discussed at PAC05[**?**]. While E163 needs low emittance, 50 pC bunches, the NLC is interested in bunches with charges up to 1 nC. To this end, the thermionic gun was replaced by a 1.6 cell, S-band RF photoinjector. Beyond the usual gun and cathode diagnostics, a low energy spectrometer (LES) allows analysis of ≤7 MeV beams with good resolution within the 1.5 m transport line between S-band cathode and X-band linac[**?**] shown in Fig. 1 below.

For E163, a new beam line exits the NLCTA at 60 MeV after two 0.9 m linac sections, a chicane and a 4-quad matching section. At this point, an exit-angle bend of 25.5° provides beam to the new area through a 6 foot shield wall. To minimize η and η' there as well as η in the quads used for this, a symmetric, two-bend dogleg with two enclosed quad triplets allows a good match from the linac to be relayed to the laser-electron IP via a doublet for matching and a conventional final focus triplet. For spots smaller than ~25 μm (nominal emittances), one can add a permanent magnet triplet nearer the IP. After the IP, a high resolving power, high energy spectrometer (HES) analyzes the perturbed electron bunches. The overall layout is shown in more detail in Fig. 1 of Ref.[**?**].

* Supported by U.S. Dept. of Energy contract DE-AC02-76SF00515.
† jus@slac.stanford.edu

A summary of the experimental requirements for E163 is given in Table I. The most demanding of these are the energy spread and timing jitter for the small modulation of the electron energy expected from the laser and the timing overlap between electron and laser beams[**?**]. Maintaining a low, RF induced energy spread in the linac requires short bunches of order 0.1 mm (0.4 psec or 1-2°X-band). Obtaining these from an RF gun is straightforward at the reduced charges for E163 but we still expect observable space charge effects for essentially all of the bunch charges of interest.

Table I: E163 Characteristics and Parameters.

Beam Energy E [MeV]	5 at Source; 60 at Expt.
Rep. Rate $f_{\rm rep}$[Hz]	10
Bunch Charge N_B[nC]	0.005 – 1.0
Emittance ϵ_{xN}; ϵ_{yN} $[10^{-6}{\rm m}]$	≤ 5.0 ; ≤ 2.5
Energy Spread $\delta E_{rms}/E$[%] (Collimator=115μm)	0.060(50 pC) 0.015(20 pC)
RMS Bunch Length[ps]	0.4(0.05 nC) 1.8(0.25 nC)
Charge Stability	±2.5 % pulse-to-pulse
RMS Timing Jitter [ps]	0.25
LES Resolving Power	4000
HES Resolving Power	20000
Photoinjector	1.6 Cell, S-band
Drive Laser	Ti:Sa(1 mJ)
Source RF System S-band(2.856 GHz)	SLAC 5045 Klystron Solid State Modulator
Injector Linac X-band(11.424 GHz)	Two 0.9 m sections 30 MV/m structures

Beam dynamics studies are separated into those used to understand the production and control of low energy-spread beams from the NLCTA and those to validate transport and matching of the beams to the experiment for a range of charges. Detailed simulations for the NLCTA with RF gun were completed through the NLCTA and E163 beamlines using the computer codes Parmela[**?**], Transport[**?**] and Elegant[**?**]. These systems posed several challenges: injection from an S-band gun into an X-band linac requires higher density bunches than typically optimal to suppress RF-induced emittance growth; the NLCTA chicane is a 3π phase advance design permitting a range of temporal dispersions (R56) but at the expense of strong, horizontal, second-order aberrations; similarly, extraction uses a 25.5° dogleg with strong space constraints requiring careful matching and control of high-order temporal and spatial dispersion (T566,T166 etc.) to preserve the phase space of potentially higher charged bunches.

SYSTEM SENSITIVITY AND STABILITY

There are many potential problem sources, beginning at the gun and running the length of the NLCTA to the large angle extraction bend separating the NLCTA from the E163 line. Directly after that, a 6-foot concrete shielding wall separates the experimental hall from the accelerator. Pre-existing location constraints produced a large separation between optical elements on either side. This is a major source of sensitivity for the quad settings. A related problem is the extraction dogleg magnet stability. Also, because of the large range of configurations that are available, and thereby magnet currents, this is another potential source of quadrupole supply instabilities. Many concerns were addressed with the supplies and their current shunts or transductors. Variations in the large-angle, dogleg supply may result in beam loss in the dogleg section, depending on their magnitude and the configuration but these were found not to affect the experiment at the IP or HES focal plane for variations of ≤1 % due to the large demagnifications there.

In Table I, a collimator in the NLCTA chicane can be used to reduce the predicted energy spread from the linac (0.06%) and clip the emittance tails. Emittances were reduced by a factor of two for a 6-fold reduction in energy spread. The reference design and many characteristics in Table I are discussed in Ref.[**?**]. The bunch length was set by the laser to have σ_t=0.4 ps (1.6° X-band), truncated at $\pm\ 2\sigma_t$. The RF gun phase is 30° (S) after zero-crossing to provide strong bunching with a nominal gradient of 42.6 MV/m (surface field 105 MV/m). This is achieved using the LES to set energy and minimize energy spread. Space charge still increases the energy spread to about 0.8% as the 5 MeV beam coasts between the gun and first linac. The phases in the two linac sections are set so electron acceleration occurs ahead of the crest, resulting in a reduction of energy spread to 0.06% during acceleration to 60 MeV.

In Table II, sensitivity to changes in control and beam parameters were done for a reference design using N_B=50 pC. Space charge affects these in various ways[**?**].

Table II: E163/NLCTA Sensitivities for Table I baseline.

Derivative-Dimensionless	Sensitivity*
$\delta\sigma_r/\delta B{\cdot}(B/\sigma_r)$	-4$_1$, -12$_2$,-25$_i$,-12$_o$
$\delta\epsilon_n/\delta B{\cdot}(B/\epsilon_n)$	-7 $B(\updownarrow)$
$\delta\sigma_{E_o}/\delta B{\cdot}(B/\sigma_{E_o})$	13 for $B(\uparrow)$
$\delta\sigma_{E_o}/\delta\sigma_r^L{\cdot}(\sigma_r^L/\sigma_{E_o})$	-1 for σ_r^L ($\downarrow$)
$\delta\sigma_{E_o}/\delta\sigma_t^L{\cdot}(\sigma_t^L/\sigma_{E_o})$	1 for σ_t^L ($\uparrow$)
$\delta\sigma_{E_o}/\delta N_B{\cdot}(N_B/\sigma_{E_o})$	2 for N_B ($\uparrow$)
$\delta E_o/\delta\phi_G/E_o$	.15%/1°S($\uparrow$);-.35%/1°S($\downarrow$)
$\delta\sigma_{E_o}/\lvert\delta\phi_G\rvert{\cdot}(\phi_G/\sigma_{E_o})$	57
$\delta\phi/\delta\phi_G$ (linac arrival ϕ)	3°(X)/1°(S)
$\delta E_o/\delta G_G{\cdot}(G_G/E_o)$	0.017 (G_G≡Gun gradient)
$\delta\sigma_{E_o}/\lvert\delta G_G\rvert{\cdot}(G_G/\sigma_{E_o})$	180
$\delta E_o/\delta G_l{\cdot}(G_l/E_o)$	0.45 (G_l≡linac gradient)

*Values are at linac exit (o) – otherwise at screen 1, 2 or linac entrance i. Derivatives are for increasing ≡($\uparrow$), decreasing ≡($\downarrow$) or symmetric ≡($\updownarrow$). No direction arrow implies insensitivity to that direction or symmetric.

The solenoid focusing field ($B\sim$2 kG) is adjusted to make the beam converge into the first linac, while simultaneously adjusting the linac phases to trade off transverse emittance for a smaller energy spread. From Table II, outgoing energy spread increases 13% for a 1% increase in *B*. It influences space charge effects in all dimensions and for all N_B of interest[**?**]. Similarly, a 1% decrease in the laser spot size (σ_r^L=0.25 cm on the cathode) increases the outgoing energy spread σ_{E_o} by 1%. Locations in Table II are shown in Fig. 1. Linac injection is (i) but linac exit (o) is not shown.

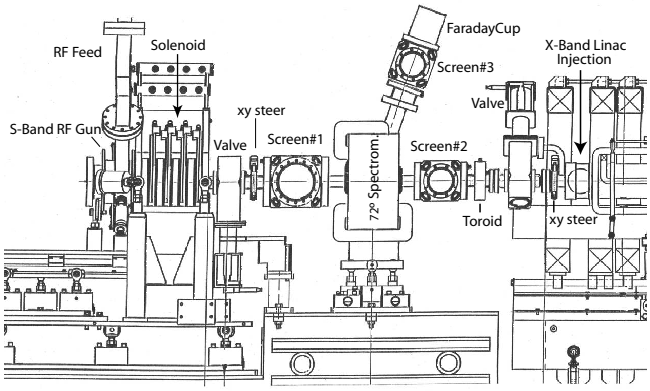

Figure 1: Layout of the SLAC E163 RF photoinjector line.

COMMISSIONING & TUNING STUDIES

The 50 pC, 60 MeV bunch out of the linac (o), before the chicane, is predicted to be round with σ_r=0.6 mm, σ_z=0.16 mm and δ=0.06 % at Screen#4 (S4) in Table III. This matches the cathode spot *and* the converging beam spot at linac entrance (i) *after* S2 and S9. Between the first and second linac sections, the beam reaches a minimum at S3. Note that several screens are not at their ideal locations or the symmetries would be more apparent in Table III.

Table III: Sizes & Protocols through NLCTA/E163.

Screen #	σ_x [mm]	σ_y [mm]	η_x[m]
1 (PROF330)	1.60	1.60	–
2 (PROF340)	1.15	1.15	–
3 (PROF430)	0.25	0.25	
4 (PROF505)	0.60	0.60	–
5 (PROF585)	1.20	0.25	–
6 (PROF790)	0.40	0.60	-0.30
9 (PROF1135)	0.80	0.80	–
10 (PROF4027)	0.44	1.80	-0.25
12 (PROF4205)	0.85	0.85	–
13 (PROF4250)	0.81	1.65	–
14 Inter. Point	0.05	0.05	–
15 Focal Plane	0.53	2.70	0.88

After S4, there is a four quad matching section in front of the NLCTA chicane. S6 is just past the middle of the chicane, directly after the collimator used to clip energy spread. At the chicane exit, another four quad matching section is followed by screen S9 at the object of the dogleg and the E163 line. This roughly mirrors S4 *and* the image of the dogleg *near* S12. These symmetries serve several functions and should simplify tuning as discussed next.

Spectrometer Systems Besides the LES and HES, several systems in between these can be thought of as prospective spectrometers[**?**] and can be tuned in that way beginning with the first dogleg section of the NLCTA chicane using screens S4, 5 & 6, nearby toroids and BPMs. The centroid of the collimator determines the dispersion and mean beam energy for a given bend strength but the jaws should not be symmetrically located about the design axis of the adjacent BPMs. The preceding triplet can be tuned for a minimum, first-order, monochromatic spot. From Tables I-III, one sees that the resolving power at the collimator is then dispersion dominated above 100 μm.

Hardware Systems Beyond the usual toroids, BPMs and profile screens at key points along the line as well as phototubes for timing and loss monitoring, a fiber optic loss line (FOLL)[**?**] was strung along the complete path of the electrons from the gun to the HES dump that is especially useful. The fiber was terminated with a miniature Hitachi phototube near the cathode that was triggered with a gun timing pulse to give typical scope traces such as shown in Fig. 2 for high charge. The resolution of this version varies slightly along the length but the leading edge is sufficient to localize beam loss to within a foot or two based on knowing the acceptance of the system, use of steering or inserting screens. The strong structure begins near S3 between linac sections. The fine structure around the strongest peak is associated with limited acceptance beam tubes (5/8in OD) near high beta quads in the chicane with short, external, wrap-around shadow collimators to protect downstream magnet coils. These are useful for dark current surviving the linac. The small peak before the HES/Dump structure is from the high-beta, final focus triplet.

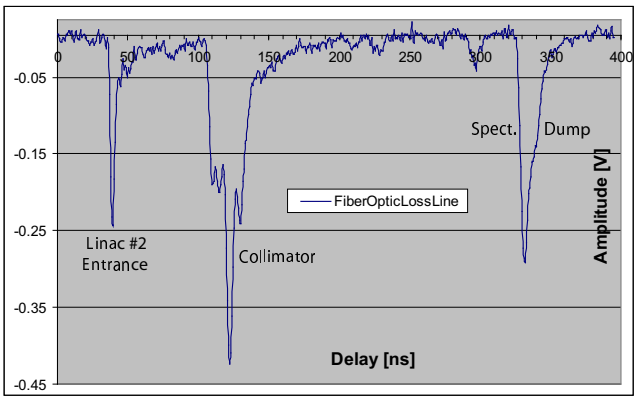

Figure 2: Trace of Fiber Optic Loss Line (FOLL) running from the NLCTA injector to the E163 spectrometer dump.

Quad Tuning There are 4 matching and eleven E163 quads – each with two trim windings that can be wired as dipole or quadrupole. The dogleg triplets are matched in series, as are the dogleg bends, to emphasize symmetry about the midpoint of this section and to minimize η=$\eta\prime$=0 at the exit before the matching doublet Q7 & Q8. One can check which are most effective and independent in both planes for any function, location or configuration.

Because many quads may be used for steering, there is a good global correction for hysteresis or steering errors[**?**] e.g. to minimize β_o and α_o at some output location (o) or, since spots at the IP or FP are often critical we find for Q7:

$$\frac{\delta\sigma_x^{IP}}{\delta k_7}\cdot\frac{k_7}{\sigma_x}=4.7 \quad \text{and} \quad \frac{\delta\sigma_y^{IP}}{\delta k_7}\cdot\frac{k_7}{\sigma_y}=-51.6 \qquad (1)$$

STATUS

All hardware has been commissioned and E163 and the NLCTA are running compatibly. A loss diagnostic line was added and screen S4 to leverage the symmetry about the collimator with S9. History buffers were used to troubleshoot beam and hardware stability. Optics have not been fully tested at the lowest emittances or energy spreads but have matched predictions of ≈0.06 % for ≈50 pC bunches without collimation. For the current minimum collimator aperture and optics we are still dispersion dominated at the HES focal plane. Because we have not run with the ideal laser profile, it is necessary to scale the expected profiles along the line using Tables II & III. Resolving power of the collimator, its physical limits, the shape and size of the laser on the cathode, reduction in dark current and RF stabilty are current concerns. IFEL based laser electron interactions have been done with 80 keV FWHM modulation.

ACKNOWLEDGMENTS

The authors thank Bruno Brugnoletti, Allan Freese, Tony Gromme, Rick Iverson, J.J. Lipari, Mike Racine, Ron Rogers, Nancy Spencer, Dieter Walz, Mark Woodley, the magnetic measurements, metrology, vacuum groups and esp. Justin May, Keith Jobe, Tonee Smith and Rich Swent.

REFERENCES

[1] R. Ruth, et al., "The Next Linear Collider Test Accelerator", PAC1993, Washington, D.C., May 1993. For complete report: SLAC-PUB-6293, July 1993.

[2] E. Colby, et al., "Beam Dynamics Studies for a Laser Acceleration Experiment", PAC2005, Knoxville, TN, May 2005.

[3] T. Plettner, et al., "Visible Laser Acceleration of Relativistic Electrons in Semi-Infinite Vacuum", Phys.Rev.Lett 95,134802(2005).

[4] H. S. Deavon, et al., LA-UR-90-1766, p. 137 (1990).

[5] D.C. Carey, et al., "Third-Order Transport", SLAC-R-95-462, May 1995

[6] M. Borland, "Elegant", APS LS-287, Sept. (2000) and M. Borland et al., PAC2003, Portland, OR, May 2003.

[7] J. Spencer, et al., "The SLAC NLC Extraction and Diagnostic Line", PAC1995, Dallas, TX, May 1995.

[8] E1000 plastic from Fiber Optic Products, Inc. of Clearlake Oaks, CA 95423 is described as 1mm plastic fiber with a black polyethylene jacket that has been around since the 60's with Specs: -55 to 85 C, dB/M= 0.15, N.A = .46 and total diameter 2.3 mm. Some possible ways to improve this setup are to add another phototube or a duplex cable (E2000 is the dual fiber equivalent). We have seen no obvious damage to the cable although it is inexpensive and easily replaced.